DNA Computation in Mammalian Cells: microRNA Logic Operations.

ARTICLE *in* JOURNAL OF THE AMERICAN CHEMICAL SOCIETY · JUNE 2013

Impact Factor: 12.11 · DOI: 10.1021/ja404350s · Source: PubMed

JACS
JOURNAL OF THE AMERICAN CHEMICAL SOCIETY

Article

pubs.acs.org/JACS

DNA Computation in Mammalian Cells: MicroRNA Logic Operations

James Hemphill and Alexander Deiters*

Department of Chemistry, North Carolina State University, Raleigh, North Carolina 27695, United States

Supporting Information

ABSTRACT: DNA computation can utilize logic gates as modules to create molecular computers with biological inputs. Modular circuits that recognize nucleic acid inputs through strand hybridization activate computation cascades to produce controlled outputs. This allows for the construction of synthetic circuits that can be interfaced with cellular environments. We have engineered oligonucleotide AND gates to respond to specific microRNA (miRNA) inputs in live mammalian cells. Both single and dual-sensing miRNA-based computation devices were synthesized for the cell-specific identification of endogenous miR-21 and miR-122. A logic gate response was observed with miRNA expression regulators, exhibiting molecular recognition of miRNA profile changes. Nucleic acid logic gates that are functional in a cellular environment and recognize endogenous inputs significantly expand the potential of DNA computation to monitor, image, and respond to cell-specific markers.

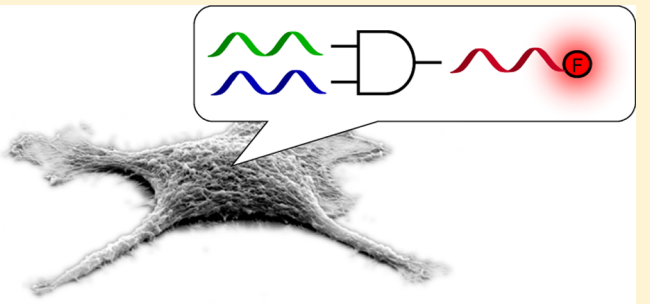

INTRODUCTION

DNA computation recognizes nucleic acid components for the construction of synthetic circuits, as DNA scaffolds and secondary structures generate output signals through sequence specific interactions with input strands. Since Adleman's molecular computer encoded the solution to a Hamiltonian path problem in DNA,[1] several developments and applications of DNA computation have been reported.[2,3] It has been estimated that DNA computation can operate at over 100 teraflops as well as store a single bit of information in one cubic nanometer, with speed and storage capacities greatly exceeding silicon computation devices.[4] Though DNA computation will never obviate the use of silicon technology due to scale limitations, its potential will be revealed through the development of in vivo computation and its application in biological synthetic circuitry.[4] Previous uses of nucleic acid based logic gates in biological systems include cellular targeted delivery,[5] RNA network gates targeting mRNA,[6] pH sensing in *Caenorhabditis elegans*,[7] and RNAi logic gates with gene expression outputs.[8−10] However, synthetic DNA-based logic gates have not yet been reported in live mammalian cells and hold great promise for the computation of endogenous biological inputs independent of protein components and gene expression systems.

DNA computation devices can produce a chemical output through toe-hold mediated strand exchange, in which toe-holds are designed to interact with specific sequences as biological inputs to displace oligonucleotides from logic gate structures.[11] Multiple DNA logic gates can be connected into complex signaling cascades to develop synthetic circuits based on nucleic acid hybridization,[12,13] which has been applied to the creation of an artificial neural network.[14] These enzyme-free nucleic acid computation devices can recognize biomolecular inputs, such as single-stranded DNA or RNA, and produce fluorescent outputs that can be easily monitored, effectively converting nucleic acid sequences into an electronic signal via an optical response.

MicroRNAs are small noncoding ssRNAs that down-regulate gene expression in a sequence specific fashion by binding the 3′ untranslated regions of target mRNAs,[15] and it has been estimated up to 30% of all genes are regulated by miRNAs.[16] The expression and misregulation of certain miRNAs has been linked to a wide range of human diseases,[17−20] highlighting the importance in understanding miRNA regulation and function.[21,22]

We demonstrate that logic gates can be used to detect miRNAs in vivo through DNA computation and will enable cell-specific gate activation based on endogenous miRNA expression patterns. Although DNA-hydridization probes have been used to detect cellular miRNAs,[23] for example, through miRNA specific molecular beacons,[24,25] DNA computation in live cells allows for Boolean logic gate operations with miRNA inputs, and the generated oligonucleotide outputs enable applications beyond miRNA pattern detection. While a previous example of miRNA detection by logic gate operations in live cells requires plasmid constructs for the expression of protein gate components,[8,9] the use of DNA logic gates to identify endogenous miRNA patterns as described here is independent of the cellular transcription and translation machinery and does not require the transfer of genetic information, allowing the circuits to be orders of magnitude smaller in size based on DNA sequence (e.g., 268 bp versus >7000 bp for a dual-miRNA input gate).

Received: May 1, 2013

   dx.doi.org/10.1021/ja404350s | J. Am. Chem. Soc. XXXX, XXX, XXX−XXX

MicroRNAs miR-21 and miR-122 were selected as inputs for miRNA-specific intracellular logic gate activation. Overexpression of miR-21 is observed in many cancer types,[26−28] while miR-122 is involved in hepatocellular carcinoma[29] and hepatitis C virus replication.[30] The DNA-based AND gate is derived from a design by Seelig et al.[11] and computes two input strands that initiate toe-hold mediated strand exchange, displacing a quencher and fluorophore duplex, leading to a fluorescent output (Supporting Information Figure 1). The use of mature miRNAs as endogenous AND gate inputs is both sequence- and cell-specific. Additionally, the fluorescent output can be observed without the need to perform cell lysis or RNA purification, which can introduce variability between experiments.[31,32] Here, the developed methodology was applied to the detection of cellular miRNA expression patterns, utilizing DNA computation as a method for the development of synthetic circuits that are functional in live cells.

RESULTS AND DISCUSSION

Photochemical Activation of Logic Gate Function in Mammalian Cells. In order to visualize DNA computation in a cellular system, we first utilized a photochemically activated logic gate, in order to have the ability to trigger toe-hold mediated strand exchange and gate output at a defined time-point. We have previously applied photocaging to the spatiotemporal control of DNA computation and the precise light-activation of nucleic acid hybridization.[33] The caging of oligonucleotides has also been used for photochemical control of gene expression through triplex-forming transcriptional regulators,[34] antisense technology,[35−39] RNA interference,[40−43] and miRNA antagomirs[44] with high spatial and temporal control in cellular environments. First, the light-triggered DNA logic gate (oligonucleotide sequences can be found in Supporting Information Table 1) was tested for activity in mammalian cells through transfection of the AND gate components into HEK293T cells. The noncaged A and B strands were used to determine if gate components would remain stable within live cells, and if activated gate fluorescence could be observed in vivo (Supporting Information Figure 2). Logic gate activation was observed 4 h after transfection and was dependent on the presence of both input strands, confirming cellular stability of the AND gate duplex and fluorescent imaging of DNA computation through standard microscopy techniques. To ensure that the logic gate could be triggered inside a cellular environment and to demonstrate intracellular toe-hold mediate strand exchange without activation in preceding mixing steps, photochemical control of DNA computation was used. The AND gate was cotransfected with the caged A_{4T} input, and irradiation (5 min, 365 nm) was performed after gate transfection was completed, followed by cellular imaging one hour later (Figure 1). Successful cellular activation of the AND gate through UV decaging of the input strand with minimal background was observed. Control experiments involving UV irradiation of the logic gate complex in the absence of a caged input strand did not show any gate degradation or fluorescence increase in vitro or in vivo (data not shown).[33] This temporal control over oligonucleotide hybridization confirms that DNA computation based on toe-hold mediated strand exchange can be conducted in live cells, since only logic gates that were successfully transfected into the cells and also exposed to UV irradiation were activated.

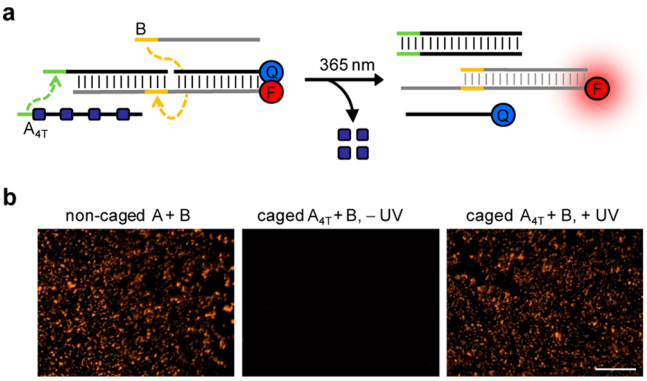

Figure 1. Photochemically controlled DNA-based AND gate activation in HEK293T cells. (a) Simplified schematic of the light-activated AND gate with a caged A_{4T} strand. NPOM-caged thymidine nucleotides (Supporting Information Figure 7a) are indicated as dark blue boxes. Toe-hold regions are shown for the A (green) and B (orange) input activation cascades, along with corresponding arrows representing hybridization steps. (b) Cells were transfected with the AND gate and A/B inputs then imaged for TAMRA fluorescent output after 4 h. Cells were also transfected with the AND gate and caged A_{4T}/B strands for 4 h then UV irradiated and imaged 1 h after exposure. Scale bar indicates 200 μm.

DNA Logic Gate Activation with Endogenous miR-21. In order to develop a DNA logic gate that can respond to an endogenous cellular activator, we engineered a miR-21-based AND gate that replaces the A input with mature miR-21. The gate sequences were amended to add miR-21 relevant toe-hold regions on G_T and recognition sites within the gate complex, which required an 8 base truncation from the AND gate duplex to accommodate the smaller miR-21 input (Supporting Information Table 2). The B strand was altered to have a toe-hold recognition sequence that is complementary to the 3′ sequence of miR-21. Additionally, the fluorophore and quencher moieties were switched to the opposite strands to increase DNA synthesis yields. To verify that toe-hold mediated strand exchange was not inhibited by the alterations in gate sequence and introduction of ssRNA as an input, the miR-21 AND gate duplex was purified and incubated with synthetic miR-21 and B_{21} strands (Figure 2b). The miR-21 AND gate is only activated when both the miR-21 and B_{21} inputs are present, providing a miR-21 responsive DNA computation device.

The miR-21-based AND gate was then tested for function in HEK293T cells, which display low endogenous expression levels of miR-21.[45] As expected, the logic gate was confirmed to produce an output signal dependent upon transfection of both synthetic miR-21 RNA and B_{21} stands (Supporting Information Figure 3). Importantly, no background fluorescence was observed with the AND gate alone or with only a single input strand, confirming the gate duplex stability in vivo. Next, two human cell lines which express high levels of miR-21 (Hela and Huh7; >10-fold increase in relative miR-21 concentration compared to the control HEK293T cells)[45] were transfected with the AND gate components in order to test detection of endogenous miR-21 through DNA computation. Experiments with these cell lines were performed in the absence of synthetic miR-21, and the AND gate was cotransfected with only the B_{21} input strand, followed by fluorescence imaging after 4 h (Figure 2c). The miR-21 AND gate duplex was not activated in the absence of B_{21}, and activation in the presence of B_{21} indicates

dx.doi.org/10.1021/ja404350s | J. Am. Chem. Soc. XXXX, XXX, XXX−XXX

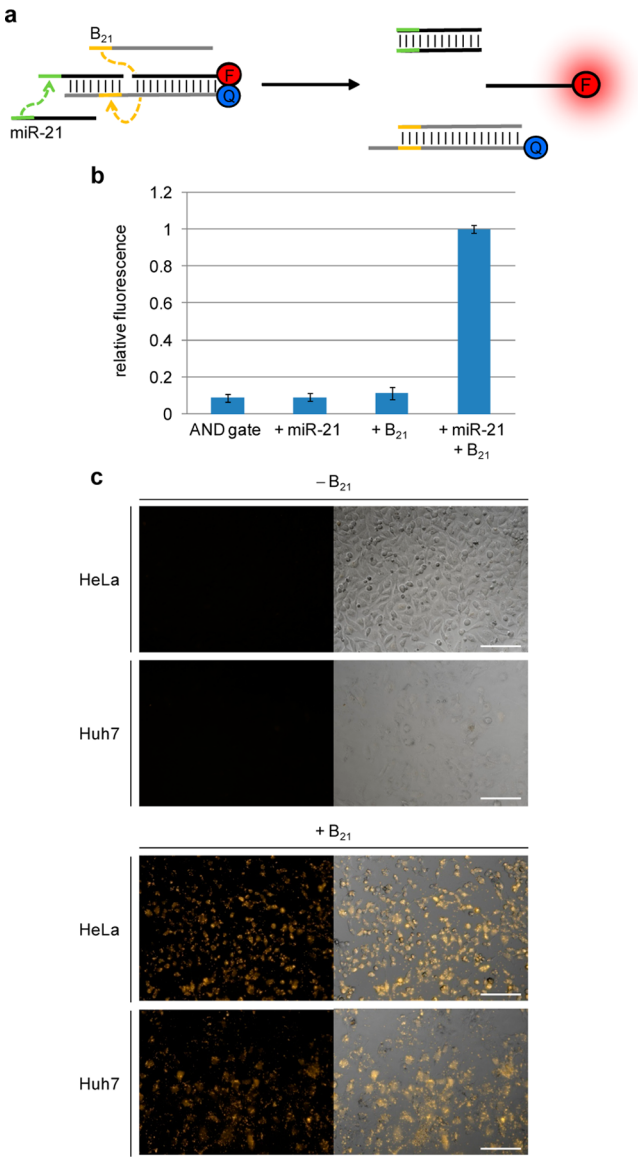

Figure 2. Engineered miR-21-based AND gate for detection of endogenous miR-21 in HeLa and Huh7 cells. (a) Simplified schematic of the AND gate. Toe-hold regions are shown for the miR-21 (green) and B_{21} (orange) input activation cascades, along with corresponding arrows representing hybridization steps. (b) The logic gate was tested for activation with miR-21 and B_{21} strands. TAMRA fluorescence was observed at 4 h and normalized to the activated AND gate. An average of three independent experiments is shown and error bars represent standard deviations. The miR-21 AND gate requires both inputs for generation of fluorescent output. (c) HeLa (top) and Huh7 (bottom) cells were transfected with the miR-21 gate and B_{21} strand then imaged after 4 h. Scale bar indicates 200 μm.

that toe-hold mediated strand exchange was initiated with endogenous miR-21 as the input strand. The presence of miR-21 with the engineered AND gate was observed in both cell lines, validating the application of AND gates for the detection of miRNA in mammalian cells. The logic gates show high transfection and activation efficiency in a cellular monolayer, as >90% of the cells show a fluorescent output from endogenous gate/miRNA interactions. A transfection time course was performed in order to determine the minimum amount of time required for AND gate activation in vivo, and early detection of miR-21 can be observed in >50% of the cells after only 1.5 h, suggesting that a short cellular incubation is sufficient for computation of miRNA expression patterns (Supporting Information Figure 4). Moreover, endogenous miRNA-driven logic gate activation was observed after an extended incubation time, showing stability of the nonactivated gate duplex in HeLa cells up to 24 h (Supporting Information Figure 5). Additional imaging experiments were performed through counter staining to identify the location of the Boolean computation event (Supporting Information Figure 6). Apparent localization of activated miR-21 logic gates could be observed around the nuclear periphery, suggesting that DNA logic gates can potentially be applied to the spatial identification of miRNA-rich and/or logic gate-rich areas. The use of logic gates to detect and image the presence of miRNAs in mammalian cells is fast, sequence specific, and does not require cell lysis and RNA purification.

Photochemical Activation of the miR-21 AND Gate. We then altered the miR-21 logic gate to be photochemically controlled through UV activation of a caged input strand. Light-activation allows for controlled cellular interaction of the logic gate output and enables temporally distinct detection of endogenous nucleic acids. A caged B_{21-4T} strand gate was synthesized with four light cleavable NPOM-dT bases (Supporting Figure 7a) and tested for the photochemical activation of the miR-21 AND gate (Figure 3b). An increase in gate fluorescent output was observed after a 5 min UV irradiation when the AND gate was analyzed in solution. The caged miR-21 AND gate was then transfected into HeLa cells for photochemically activated miRNA detection (Figure 3c). As expected, in conjunction with the caged B_{21-4T} strand, the miR-21 AND gate only detects endogenous miR-21 after UV exposure. The combination of photocaging and miRNA detection allows for the use of light as a second input when analyzing endogenous miRNA expression in biological environments.

Logic Gate Response to Environmental Effects on miRNA Regulation. Environmental changes can greatly affect miRNA expression patterns and quickly monitoring these effects with DNA computation devices has potential in diagnostic application and therapeutic responses. Here, the AND gate was applied to the detection of changes in miR-21 levels in HeLa cells through both small molecule treatment with a miR-21 inhibiting azobenzene[46] (Supporting Information Figure 7b) and antagomir treatment with a reverse complement of the mature miR-21 sequence,[47] perturbing different stages of the miRNA pathway.[48] Cells were treated with either the small molecule or the miR-21 antagomir for 48 h, followed by transfection of the miR-21 AND gate and subsequent fluorescence imaging (Figure 4). The logic gate output is deactivated through treatment with either the small molecule or the miRNA antagomir, demonstrating successful DNA computation of miRNA responses to environmental changes. A dose–response experiment was performed to observe the effects of decreased small molecule concentrations on detection of miR-21 inhibition (Supporting Information Figure 8), and detection has been shown to be sensitive to miRNA inhibitors at submicromolar concentrations, comparable to genetically encoded luciferase reporters.[49]

DNA Logic Gate Activation with Endogenous miR-122. In order to demonstrate the general applicability of sequence-specific DNA logic gates for the detection of various miRNAs in different cellular environments, a miR-122-based AND gate was engineered. The miR-122 AND gate was

dx.doi.org/10.1021/ja404350s | J. Am. Chem. Soc. XXXX, XXX, XXX–XXX

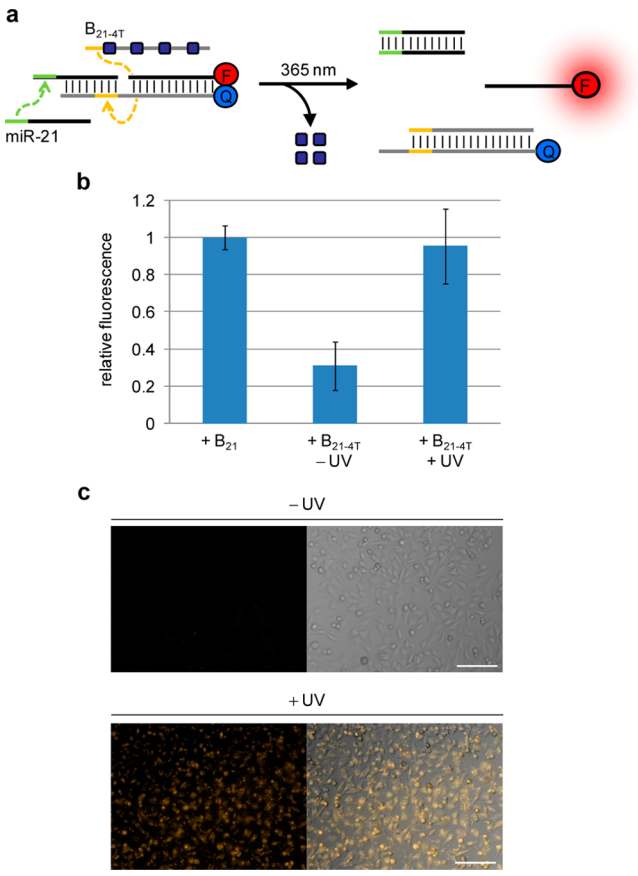

Figure 3. A photochemically triggered miR-21 AND gate only detects endogenous miR-21 after irradiation. (a) Simplified schematic of the AND gate with a caged B_{21-4T} strand. NPOM-caged thymidine nucleotides (Supporting Information Figure 7a) are indicated as dark blue boxes. Toe-hold regions are shown for the miR-21 (green) and B_{21-4T} (orange) input activation cascades, along with corresponding arrows representing hybridization steps. (b) The AND gate was tested for photochemical (365 nm, 5 min) activation of caged B_{21-4T}. TAMRA fluorescence was observed at 4 h and normalized to the noncaged activated AND gate. An average of three independent experiments is shown and error bars represent standard deviations. (c) HeLa cells were cotransfected with the miR-21 gate and caged B_{21-4T} for 4 h and then UV irradiated and imaged 1 h after exposure. Scale bar indicates 200 μm.

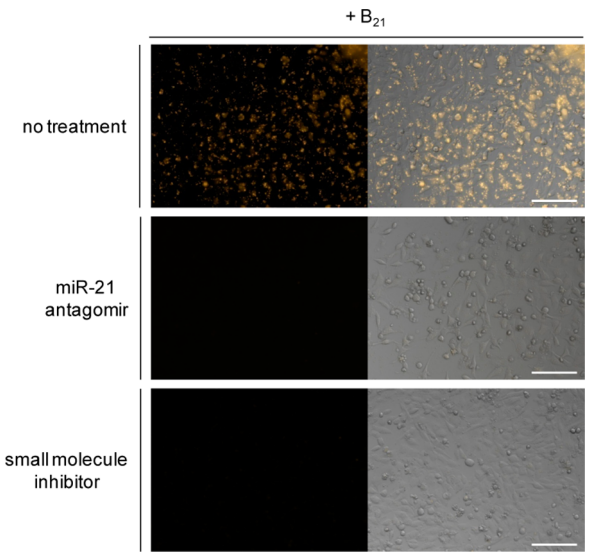

Figure 4. Application of the miR-21 AND gate to the detection of functionally depleted miR-21 in HeLa cells due to antagomir or small molecule treatment. Cells were treated for 48 h with a miR-21 antagomir or a miR-21 small molecule inhibitor (Supporting Information Figure 7b) followed by cotransfection with the miR-21 gate and B_{21} as previously described. Scale bar indicates 200 μm.

designed through reconfiguration of the two input logic gate system (Supporting Information Table 3) and confirmed to be activated in the presence of both miR-122 RNA and B_{122} inputs (Figure 5b). No background fluorescence was observed in HEK293T or HeLa cells, which do not express miR-122,[45] and logic gate function was specifically activated through the addition of synthetic miR-122 (Supporting Information Figures 9 and 10). To validate endogenous cellular activation, the miR-122 AND gate was applied to Huh7 cells, which express high levels of miR-122 (>10-fold increase in relative miR-122 concentrations compared to the control HEK293T and HeLa cells).[45] Efficient logic gate activation was observed in the presence of cellular miR-122 and the addition of the second B_{122} input strand (Figure 5c). These experiments confirm that the AND gate design can be readily altered to recognize different miRNAs, in different cell types, and can be applied to the imaging of cell-specific miRNA markers.

DNA Logic Gate Computation of Two Endogenous miRNA Inputs. A distinct application of DNA logic gates that are functional in cellular computation events is the ability to trigger an output signal dependent upon the recognition of multiple endogenous inputs. Expression patterns of miRNAs associated with cancer and other disease states often involve the simultaneous up-and-down regulation of several miRNAs,[48] highlighting the importance of simultaneous detection for the computation of diagnostic and therapeutic outputs based on miRNA expression patterns. In order to develop a dual-miRNA logic gate, we adapted the design of translator gates[11] that were engineered to interact with miR-21 and miR-122 inputs (Supporting Information Table 4 and Supporting Figure 11), converting them into DNA output strands that subsequently trigger AND gate activation and fluorescent output. This modular design will allow for the general application of the cellular DNA logic gate system for dual-miRNA activation through simple tailoring of the connected translator subcircuits to any two miRNA inputs. The miR-21/122 AND gate system was first tested with synthetic RNA molecules and was only activated in the presence of both miRNAs (Figure 6b). Cellular transfections of the AND gate and the two translator gates were then tested in HEK293T cells as they lack miR-21 and miR-122,[45] thereby enabling conditional gate activation through treatment with synthetic miRNA mimics. These experiments validated that the translator-coupled AND gate circuit maintains a low fluorescence background, remains stable intracellularly, and is activated only in the presence of both synthetic miRNAs (Supporting Information Figure 12). Moreover, in HeLa cells that endogenously express miR-21 but not miR-122,[45] the addition of synthetic miR-122 was sufficient for gate activation demonstrating that dual-sensing miRNA gates can be activated with an endogenous miRNA input (Supporting Information Figure 13). Finally, the translator-coupled AND gate device was successfully applied in Huh7 cells, which express high functional levels of both miRNAs,[45,50] thus displaying a rapid Boolean operation with endogenous miR-21 and miR-122 as inputs (Figure 6c). Both translator gate interactions were required to trigger the AND

dx.doi.org/10.1021/ja404350s | J. Am. Chem. Soc. XXXX, XXX, XXX–XXX

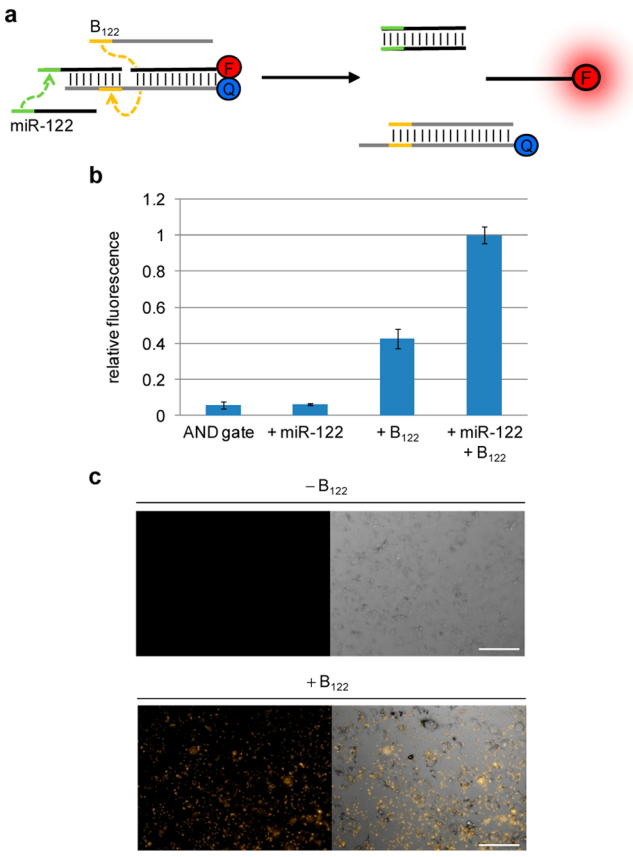

Figure 5. Engineered miR-122-based AND gate. (a) Simplified schematic of the AND gate. Toe-hold regions are shown for the miR-122 (green) and B_{122} (orange) input activation cascades, along with corresponding arrows representing hybridization steps. (b) The logic gate was tested for activation with miR-122 and B_{122} strands. TAMRA fluorescence was observed at 4 h and normalized to the activated AND gate. An average of three independent experiments is shown and error bars represent standard deviations. (c) Huh7 cells were cotransfected with the miR-122 gate and B_{122} strand and imaged after 4 h. Scale bar indicates 200 μm.

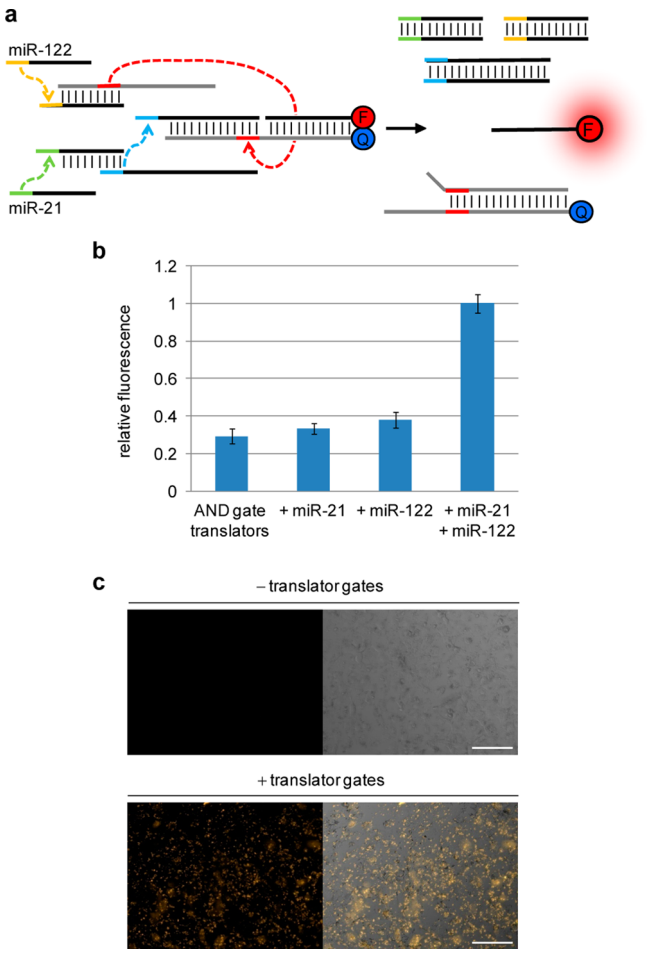

Figure 6. Engineered miR-21/122 translator-coupled AND gate enables dual detection of endogenous miRNA expression patterns. (a) Simplified schematic of the AND gate with translator gates for each miRNA. Toe-hold regions are shown for the miR-21 (green/blue) and miR-122 (orange/red) activation cascades, along with corresponding arrows representing hybridization steps. (b) The logic gate was tested for activation with the miR-21 and miR-122 RNA strands. TAMRA fluorescence was observed at 4 h and normalized to the activated AND gate. An average of three independent experiments is shown and error bars represent standard deviations. (c) Huh7 cells were cotransfected with the miR-21/122 AND gate and translator gates, followed by imaging after 4 h. Scale bar indicates 200 μm.

gate, further verifying complete specificity for the two cellular miRNA inputs (Supporting Information Figure 14).

CONCLUSION

The successful activation of DNA logic gates in live cells lays the groundwork to pursue the development of biological applications for complex molecular computation. Light-directed DNA assembly within mammalian cells was demonstrated as a stepping stone toward cellular activation of synthetic DNA computation circuits. Logic gates were developed and tested for in vivo activation of a fluorescent output dependent upon the presence of endogenous miRNAs. The cell-specific miRNA detection was achieved through DNA computation with AND gates that were engineered to recognize, with high specificity, either miR-21 or miR-122 or both miRNAs. The response of an endogenously activated logic gate was demonstrated to identify reduced miRNA function due to environmental changes, for example, exposure to miRNA small molecule inhibitors. The ability to compute the presence (or absence through the application of other Boolean logic gates) of multiple miRNAs in live cells has implications in the diagnosis and treatment (e.g., through the release of therapeutic agents) of human disease, especially cancer. Moreover, this modular computation approach can be easily reconfigured for the detection of other endogenous nucleic acid inputs. The DNA devices developed have potential application in the detection of miRNA markers for cellular expression profiling and can be expanded to the in vivo detection of other miRNAs, as well as interfaced with additional gates to develop complex DNA-based circuits that can recognize and respond to multi-miRNA patterns.

EXPERIMENTAL SECTION

Logic Gate Duplex Purification. Oligonucleotides were ordered from IDT (nonmodified) and Alpha DNA (5′ TAMRA and 3′ BHQ2 modifications). Gate complexes were formed at 20 μM in 200 μL of TAE/Mg^{2+} buffer (0.04 M tris-acetate, 1 mM ethylenediaminetetraacetic acid (EDTA), and 12.5 mM magnesium acetate) and annealed over a temperature gradient from 95 to 22 °C over 30 min. The gates were then purified with a 0.75 mm 20% native Tris-PAGE gel (200 V, 40 min). The full size duplex bands were excised and eluted overnight at 4 °C in TAE/Mg^{2+}buffer. Translator gate duplexes of strands $J_{21\ Out}$/

dx.doi.org/10.1021/ja404350s | J. Am. Chem. Soc. XXXX, XXX, XXX–XXX

K_{21} and $L_{122}/M_{122\ Out}$ were purified in the same manner. Gate concentrations were determined by UV absorption.

Gate Functional Examination. Synthetic miRNA strands were ordered from Sigma. Fluorescence was measured on a BioTek Synergy 4 plate reader (ex, 532; em, 576) in black 96-well plates (BD Falcon). The AND gates were analyzed at 200 nM with 800 nM input strands in 50 μL TAE/Mg^{2+} buffer (0.04 M tris-acetate, 1 mM EDTA, and 12.5 mM magnesium acetate). The translator gates for the miR-21/122 AND gate were used at 200 nM. Fluorescence was measured at 4 h and normalized to the positive control for each activated logic gate.

Cellular Logic Gate Transfection. Cells were seeded at ∼10 000 cell per well into black 96-well plates (BD Falcon) and incubated overnight in DMEM growth media (10% FBS, 2% penicillin/streptomycin, 37 °C, 5% CO_2). Transfections were performed using 1 μL of X-tremeGENE (Roche) in 100 μL of Opti-Mem (Invitrogen) at 37 °C for 4 h. The light-triggered AND gate was transfected at 200 nM with 800 nM input strands. The miRNA-based AND gates were transfected at 50 nM with 200 nM input strands. The miR-21/122 translator gates were also transfected at 50 nM. After 4 h, the Opti-Mem transfection mixtures were removed from the cells and replaced with clear DMEM-high modified growth media (Thermo Scientific) for imaging.

Live Cell Imaging of TAMRA Fluorescence. All cellular images were taken in brightfield as well as TAMRA fluorescent channels on a Zeiss Observer Z1 (20× objective, NA 0.8 plan-apochromat; Zeiss) and a RFP (43 HE) filter (ex, BP545/25; em, BP605/70). The TAMRA signal was normalized to a standard setting for fluorescent intensity (black = 300; white = 2000; gamma = 0.6) in Zen Pro 2011. Fluorescence merged with brightfield images are shown for each endogenously activated miRNA cellular logic gate.

Imaging of Subcellular TAMRA Fluorescence Localization. HeLa cells were seeded at ∼50 000 cell per well into 4-well chamber slides (Lab-Tek) and incubated overnight in DMEM growth media (10% FBS, 2% penicillin/streptomycin, 37 °C, 5% CO_2). The miR-21 AND gate was transfected at 50 nM with 200 nM B_{21} input strand using 5 μL of X-tremeGENE (Roche) in 1 mL of Opti-Mem (Invitrogen) at 37 °C for 4 h. After 4 h, the Opti-Mem transfection mixtures were removed and cells were fixed with 3.75% formaldehyde, followed by nuclear DAPI counter staining (Invitrogen) according to standard protocols. Fluorescence was imaged with a Zeiss Observer Z1 (63× oil objective, NA 1.4 plan-apochromat; Zeiss) using DAPI [BFP (68 HE); ex, BP377/28; em, BP464/100] and TAMRA [RFP (43 HE); ex, BP545/25; em, BP605/70] filter cubes. The TAMRA signal was normalized to a standard setting for fluorescent intensity (black = 300; white = 2000; gamma = 0.6) in Zen Pro 2011.

Specialized DNA Synthesis. DNA synthesis was performed using standard β-cyanoethyl phosphoramidite chemistry on a MerMade4 synthesizer (Bioautomation). The caged oligonucleotides were synthesized on 50 nmol solid-phase supports with commercial reagents for automated DNA synthesis (Glen Research). Synthesis cycles were provided by Bioautomation and edited to increase the base coupling time for all normal bases (30 s) and the incorporation of the modified phosphoramidite NPOM-caged thymidine (6 min). The NPOM-caged thymidine phosphoramidite was dissolved in anhydrous acetonitrile to a final concentration of 0.05 M. The full-length caged oligonucleotides were purified with Nap-10 columns (GE Healthcare) followed by PAGE gel band excision and elution into TAE/Mg^{2+}buffer. See the Logic Gate Duplex Purification subsection for specific information.

Photochemical Activation in Mammalian Cells. Transfected cells were incubated for 1 h and UV irradiated for 5 min on a 365 nm transilluminator. Cellular images were taken 1 h post UV irradiation with the same setting as previously described.

Small Molecule and Antagomir Treatment of HeLa Cells. Cells were seeded at ∼10 000 cell per well into black 96-well plates and incubated overnight in DMEM growth media (10% FBS, 2% penicillin/streptomycin, 37 °C, 5% CO_2). The cells were treated with (*E*)-4-(phenyldiazenyl)-*N*-(prop-2-yn-1-yl)benzamide (10 μM) in 1% DMSO/DMEM growth media for 48 h. The dose−response treatments were performed in 1% DMSO/DMEM at decreasing concentrations of the small molecule (as low as 10 nM). Alternatively, cells were transfected with 100 pmol of the miR-21 antagomir using 1 μL of X-tremeGENE (Roche) in 100 μL of Opti-Mem (Invitrogen) at 37 °C for 4 h. Logic gate transfections were performed after 48 h incubations as described previously.

■ ASSOCIATED CONTENT

Ⓢ Supporting Information

Detailed DNA computation schemes, sequence of DNA oligomers, fluorescence images of control experiments, expanded condition sets, and chemical structures of the caging group and small molecule inhibitor. This material is available free of charge via the Internet at http://pubs.acs.org.

■ AUTHOR INFORMATION

Corresponding Author

alex_deiters@ncsu.edu

Notes

The authors declare no competing financial interest.

■ ACKNOWLEDGMENTS

We thank Alex Prokup for initial gate preparation and helpful discussion. This research was funded in part by the Teva USA Scholars Grants Program, administered by the American Chemical Society Office of Research Grants, and by a Research Scholar Grant (120130-RSG-11-066-01-RMC) from the American Cancer Society.

■ REFERENCES

(1) Adleman, L. M. *Science* **1994**, *266*, 1021.
(2) Benenson, Y. *Nat Rev Genet* **2012**, *13*, 455.
(3) Miyamoto, T.; Razavi, S.; Derose, R.; Inoue, T. *ACS Synth. Biol.* **2013**, *2*, 72.
(4) Parker, J. *EMBO Rep.* **2003**, *4*, 7.
(5) Douglas, S. M.; Bachelet, I.; Church, G. M. *Science* **2012**, *335*, 831.
(6) Benenson, Y. *Curr. Opin. Biotechnol.* **2009**, *20*, 471.
(7) Surana, S.; Bhat, J. M.; Koushika, S. P.; Krishnan, Y. *Nat. Commun.* **2011**, *2*, 340.
(8) Rinaudo, K.; Bleris, L.; Maddamsetti, R.; Subramanian, S.; Weiss, R.; Benenson, Y. *Nat. Biotechnol.* **2007**, *25*, 795.
(9) Xie, Z.; Wroblewska, L.; Prochazka, L.; Weiss, R.; Benenson, Y. *Science* **2011**, *333*, 1307.
(10) Leisner, M.; Bleris, L.; Lohmueller, J.; Xie, Z.; Benenson, Y. *Methods Mol. Biol.* **2012**, *813*, 169.
(11) Seelig, G.; Soloveichik, D.; Zhang, D. Y.; Winfree, E. *Science* **2006**, *314*, 1585.
(12) Qian, L.; Winfree, E. *Science* **2011**, *332*, 1196.
(13) Zhang, D. Y.; Turberfield, A. J.; Yurke, B.; Winfree, E. *Science* **2007**, *318*, 1121.
(14) Qian, L.; Winfree, E.; Bruck, J. *Nature* **2011**, *475*, 368.
(15) Carthew, R. W. *Curr. Opin. Genet. Dev.* **2006**, *16*, 203.
(16) Lewis, B. P.; Burge, C. B.; Bartel, D. P. *Cell* **2005**, *120*, 15.
(17) Tong, A. W.; Nemunaitis, J. *Cancer Gene Ther.* **2008**, *15*, 341.
(18) Port, J. D.; Sucharov, C. *J. Cardiovasc. Pharmacol.* **2010**, *56*, 444.
(19) Lindsay, M. A. *Trends Immunol.* **2008**, *29*, 343.
(20) Cullen, B. R. *Genes Dev.* **2011**, *25*, 1881.
(21) Sayed, D.; Abdellatif, M. *Physiol. Rev.* **2011**, *91*, 827.
(22) Sevignani, C.; Calin, G. A.; Siracusa, L. D.; Croce, C. M. *Mamm. Genome* **2006**, *17*, 189.
(23) Wang, F.; Niu, G.; Chen, X.; Cao, F. *Eur. J. Nucl. Med. Mol. Imaging* **2011**, *38*, 1572.
(24) Yao, Q.; Zhang, A. M.; Ma, H.; Lin, S.; Wang, X. X.; Sun, J. G.; Chen, Z. T. *Mol. Cell. Probes* **2012**, *26*, 182.
(25) Kang, W. J.; Cho, Y. L.; Chae, J. R.; Lee, J. D.; Choi, K. J.; Kim, S. *Biomaterials* **2011**, *32*, 1915.

(26) Medina, P. P.; Nolde, M.; Slack, F. J. *Nature* **2010**, *467*, 86.
(27) Schetter, A. J.; Leung, S. Y.; Sohn, J. J.; Zanetti, K. A.; Bowman, E. D.; Yanaihara, N.; Yuen, S. T.; Chan, T. L.; Kwong, D. L.; Au, G. K.; Liu, C. G.; Calin, G. A.; Croce, C. M.; Harris, C. C. *JAMA, J. Am. Med. Assoc.* **2008**, *299*, 425.
(28) Zhu, S.; Wu, H.; Wu, F.; Nie, D.; Sheng, S.; Mo, Y. Y. *Cell Res.* **2008**, *18*, 350.
(29) Negrini, M.; Gramantieri, L.; Sabbioni, S.; Croce, C. M. *Anticancer Agents Med. Chem.* **2011**, *11*, 500.
(30) Jopling, C. L.; Yi, M.; Lancaster, A. M.; Lemon, S. M.; Sarnow, P. *Science* **2005**, *309*, 1577.
(31) Bustin, S. A.; Nolan, T. *J. Biomol. Tech.* **2004**, *15*, 155.
(32) Bustin, S. A. *J. Mol. Endocrinol.* **2002**, *29*, 23.
(33) Prokup, A.; Hemphill, J.; Deiters, A. *J. Am. Chem. Soc.* **2012**, *134*, 3810.
(34) Govan, J. M.; Uprety, R.; Hemphill, J.; Lively, M. O.; Deiters, A. *ACS Chem. Biol.* **2012**, *7*, 1247.
(35) Deiters, A.; Garner, R. A.; Lusic, H.; Govan, J. M.; Dush, M.; Nascone-Yoder, N. M.; Yoder, J. A. *J. Am. Chem. Soc.* **2010**, *132*, 15644.
(36) Young, D. D.; Lusic, H.; Lively, M. O.; Yoder, J. A.; Deiters, A. *Chembiochem* **2008**, *9*, 2937.
(37) Young, D. D.; Lively, M. O.; Deiters, A. *J. Am. Chem. Soc.* **2010**, *132*, 6183.
(38) Tang, X.; Swaminathan, J.; Gewirtz, A. M.; Dmochowski, I. J. *Nucleic Acids Res.* **2008**, *36*, 559.
(39) Shestopalov, I. A.; Sinha, S.; Chen, J. K. *Nat. Chem. Biol.* **2007**, *3*, 650.
(40) Shah, S.; Jain, P. K.; Kala, A.; Karunakaran, D.; Friedman, S. H. *Nucleic Acids Res.* **2009**, *37*, 4508.
(41) Blidner, R. A.; Svoboda, K. R.; Hammer, R. P.; Monroe, W. T. *Mol. BioSyst.* **2008**, *4*, 431.
(42) Mikat, V.; Heckel, A. *RNA* **2007**, *13*, 2341.
(43) Casey, J. P.; Blidner, R. A.; Monroe, W. T. *Mol Pharmaceutics* **2009**, *6*, 669.
(44) Connelly, C. M.; Uprety, R.; Hemphill, J.; Deiters, A. *Mol. BioSyst.* **2012**, *8*, 2987−2993.
(45) Tian, W.; Dong, X.; Liu, X.; Wang, G.; Dong, Z.; Shen, W.; Zheng, G.; Lu, J.; Chen, J.; Wang, Y.; Wu, Z.; Wu, X. *PLoS One* **2012**, *7*, e29551.
(46) Gumireddy, K.; Young, D. D.; Xiong, X.; Hogenesch, J. B.; Huang, Q.; Deiters, A. *Angew. Chem., Int. Ed.* **2008**, *47*, 7482.
(47) Krützfeldt, J.; Rajewsky, N.; Braich, R.; Rajeev, K. G.; Tuschl, T.; Manoharan, M.; Stoffel, M. *Nature* **2005**, *438*, 685.
(48) Liu, Z.; Sall, A.; Yang, D. *Int. J. Mol. Sci.* **2008**, *9*, 978.
(49) Connelly, C. M.; Thomas, M.; Deiters, A. *J. Biomol. Screening* **2012**, *17*, 822.
(50) Chen, H. L.; Huang, J. Y.; Chen, C. M.; Chu, T. H.; Shih, C. *PLoS One* **2012**, *7*, e34116.